

Article

# Response of Chlorophyll, Carotenoid and SPAD-502 Measurement to Salinity and Nutrient Stress in Wheat (*Triticum aestivum* L.)

Syed Haleem Shah \*, Rasmus Houborg and Matthew F. McCabe 

Water Desalination and Reuse Center, Division of Biological and Environmental Science and Engineering, King Abdullah University of Science and Technology, Thuwal 23955-6900, Saudi Arabia; Rasmus.Houborg@kaust.edu.sa (R.H.); Matthew.McCabe@kaust.edu.sa (M.F.M.)

\* Correspondence: SyedHaleem.Shah@kaust.edu.sa; Tel.: +966-12-808-4949

Academic Editor: Peter Langridge

Received: 31 July 2017; Accepted: 8 September 2017; Published: 12 September 2017

**Abstract:** Abiotic stress can alter key physiological constituents and functions in green plants. Improving the capacity to monitor this response in a non-destructive manner is of considerable interest, as it would offer a direct means of initiating timely corrective action. Given the vital role that plant pigments play in the photosynthetic process and general plant physiological condition, their accurate estimation would provide a means to monitor plant health and indirectly determine stress response. The aim of this work is to evaluate the response of leaf chlorophyll and carotenoid ( $C_t$ ) content in wheat (*Triticum aestivum* L.) to changes in varying application levels of soil salinity and fertilizer applied over a complete growth cycle. The study also seeks to establish and analyze relationships between measurements from a SPAD-502 instrument and the leaf pigments, as extracted at the anthesis stage. A greenhouse pot experiment was conducted in triplicate by employing distinct treatments of both soil salinity and fertilizer dose at three levels. Results showed that higher doses of fertilizer increased the content of leaf pigments across all levels of soil salinity. Likewise, increasing the level of soil salinity significantly increased the chlorophyll and  $C_t$  content per leaf area at all levels of applied fertilizer. However, as an adaptation process and defense mechanism under salinity stress, leaves were found to be thicker and narrower. Thus, on a per-plant basis, increasing salinity significantly reduced the chlorophyll ( $Chl_t$ ) and  $C_t$  produced under each fertilizer treatment. In addition, interaction effects of soil salinity and fertilizer application on the photosynthetic pigment content were found to be significant, as the higher amounts of fertilizer augmented the detrimental effects of salinity. A strong positive ( $R^2 = 0.93$ ) and statistically significant ( $p < 0.001$ ) relationship between SPAD-502 values and  $Chl_t$  and between SPAD-502 values and  $C_t$  content ( $R^2 = 0.85$ ) was determined based on a large ( $n = 277$ ) dataset. We demonstrate that the SPAD-502 readings and plant photosynthetic pigment content per-leaf area are profoundly affected by salinity and nutrient stress, but that the general form of their relationship remains largely unaffected by the stress. As such, a generalized regression model can be used for  $Chl_t$  and  $C_t$  estimation, even across a range of salinity and fertilizer gradients.

**Keywords:** wheat crop; SPAD measurement; chlorophyll; carotenoids; pigment; salinity stress; nutrient stress; photosynthesis

## 1. Introduction

The accurate estimation of leaf photosynthetic pigments is an important element in monitoring plant stress and fertilizer application and managing the overall vegetation health—particularly in agricultural systems, where productivity levels are directly related to plant condition. Leaf

photosynthetic pigments are key variables in characterizing photosynthetic response and gross primary production in the biosphere [1–4], with the pigments playing a central role in light harvesting, photosystem protection, and other growth functions [5–7]. Chlorophylls control the photosynthetic potential of plants by capturing light energy from the sun [8], and represent one of the most important photosynthetic pigments. The leaf chlorophyll content provides a key indicator of the photosynthetic capacity [2,9], and in combination with measurements such as leaf area index has been found to be a critical proxy for vegetation productivity [10] and prevailing stress in vegetation [11–13]. Carotenoids ( $C_t$ ) are composed of carotenes and xanthophylls, and represent another key photosynthetic pigment group. Being essential structural components of the photosynthetic antenna,  $C_t$  participate in harvesting light energy for photosynthesis [14,15]. In addition to the direct contribution in the photosynthetic process,  $C_t$  are also involved in the defense mechanism against oxidative stress [16–18], and play an essential role in the dissipation of excess light energy and provide protection to reaction centers [19–21].

Abiotic stresses arising from drought, extreme temperatures, salinity, or nutrient deficiency adversely affect the photosynthesis process in higher plants, as well as their growth and development [22–24], and thus the overall productivity of an ecosystem [25]. Photosynthetic machinery consists of various mechanisms, including gas exchange systems, photosynthetic pigments, photosystems, electron transport systems, carbon reduction pathways, and enzyme systems [26]. Any impairment to one or more of these processes would reduce the photosynthetic activity of the plants, their growth, and their biomass production. However, the nature and impact of damage resulting from stresses has been a matter of controversy among plant physiologists for many years, and the reported results vary considerably according to the plant species, conditions, and experimental procedures used in the studies [26].

Salinity stress may alter cellular and whole plant-level physiological and biochemical processes [27–29]. The immediate and direct effect of salinity is the imbalance of osmotic potential in the soil–plant system preventing water uptake by roots [30,31]. The nature of this effect is similar to drought stress [32,33]. Ion homeostasis, repressed metabolism, membrane rupture, and energy expense on defense mechanisms may also result from high levels of salinity [33,34]. The consequences of salinity stress on photosynthesis are highly complex and are attributed directly to the stomatal closure and mesophyll limitations for the diffusion of gases, which ultimately alters the net photosynthesis process [23,35]. The severity and duration of the incessant stress has a profound effect on the content of leaf photosynthetic pigments, and results in metabolic process impairment [36,37]. However, the effect of salinity on photosynthetic pigments is highly plant-specific [26] and requires further exploration to provide an improved understanding of variations resulting from salinity stress across species.

Nutrients supplied by fertilizers play a fundamental role in the structural and functional components of photosynthetic machinery [38–40], and an optimal nutrient supply is considered essential for the biosynthesis of plant photosynthetic pigments [41,42]. Any deficiencies will likely lead to a reduced content of leaf pigments, retarded plant growth, and low net primary productivity [43]. The response of plant growth and production to various essential plant nutrients has been extensively studied around the globe. Most of these studies were conducted to evaluate best nutrition management practices under non-saline conditions. However, a high concentration of salts and nutrient imbalances in the root-zone makes it difficult to examine the response of plant health to fertilizer under saline conditions [44,45]. In such conditions, a mixed response of plant yield has been reported, with some studies showing a positive response of fertilizer [46,47], while others have reported a negative [48–50] or negligible response at high salinity levels [45]. In nutrient-deficient soils, fertilizers have been seen to improve plant growth, regardless of salinity level [51].

While environmental stresses such as those described above typically reduce the chlorophyll content [52–56], some studies have reported increased chlorophyll content with increasing salinity stress in salt-tolerant plants [4,57–59]. Accordingly, higher chlorophyll accumulation is considered to be a potential indicator of salinity tolerance [60,61]. Carotenoids also provide useful insights into

the physiological state of plants under stress [62–65], and the response of  $C_t$  to stress is similar to the chlorophyll content in many plants [21,66]. They are involved in the transcriptional modulation of a large set of genes responsive to reactive oxygen species [67] and long-distance stress signaling in photosynthetic plants [68]. As a photo-protection mechanism,  $C_t$  are retained during the process of chlorophyll degeneration at leaf senescence [69,70]. In previous studies, the ratio of chlorophyll to  $C_t$  has demonstrated some utility as an indicator of plant stress [71] and plant acclimation and adaptation to environmental stresses [70].

Traditional methods of measuring photosynthetic pigments involve complex procedures of solvent extraction followed by in vitro spectrophotometric determination, which make them destructive, labor intensive, time-consuming, and expensive [72–74]. Likewise, laborious sampling and analytical procedures generally make data collection over larger space and time domains impractical. Alternatively, chlorophyll meters such as the SPAD-502 (Konica Minolta Corp., Solna, Sweden) offer a modest, fast, and non-destructive approach to determine relative values of chlorophyll content, but the meter needs to be calibrated for measurement in absolute units of chlorophyll content per unit leaf area. The relationships between SPAD readings and extractable leaf pigments in various plant species have been the focus of several studies [75–79]. Such studies indicate that the relationship is not universal and varies with measurement procedure, sensor type, leaf direction and exposure, and plant species (sometimes even within the same plant species) [80–84]. Importantly, the influence of interactions of abiotic stresses such as salinity and nutrient limitations on the relationship has received little attention.

As such, the establishment of relationships between SPAD values and absolute leaf pigment content under a controlled environment with varying levels of plant stress is an area of needed investigation. To address this knowledge gap, this study attempts to: (1) investigate the influence of both salinity and fertilizer, as well as their interaction, on photosynthetic pigments of wheat leaves at the anthesis (i.e., flowering) stage; (2) determine the relationships between SPAD-502 readings and the extractable chlorophyll ( $Chl_t$ ) and  $C_t$  under these varying conditions; and (3) evaluate the effect of salinity and nutrient stress on the coefficients of the developed regression models.

## 2. Results

### 2.1. Impact of Salinity and Fertilizer Treatments on Pigment Content

The leaf pigment content as influenced by salinity and fertilizer application is presented in two ways: (i) pigment content per unit leaf area ( $\mu\text{g}\cdot\text{cm}^{-2}$ ), and (ii) the total content of pigments produced per plant ( $\text{mg}\cdot\text{plant}^{-1}$ ), as analyzed in the following two sub-sections.

#### 2.1.1. Leaf Area-Based Pigment Content

In general, the colour of the leaves in the experimental units varied considerably from dark green to pale brown at the time of measurement. Chlorophylls were the dominant pigment in the wheat leaves and ranged from 1.5 to 66.4  $\mu\text{g}\cdot\text{cm}^{-2}$ , with chlorophyll a ( $Chl_a$ ) ranging from 0.6 to 44.3 and chlorophyll b ( $Chl_b$ ) from 0.4 to 22.3  $\mu\text{g}\cdot\text{cm}^{-2}$ . The ratio of  $Chl_a$  to  $Chl_b$  was generally around 2 under the various combined salinity and fertilizer treatments.  $C_t$  content was in the range of 0.3 to 5.8  $\mu\text{g}\cdot\text{cm}^{-2}$ . At double fertilizer dose, the lower the salinity levels, the smaller the leaf  $Chl_a$ ; i.e., at 7  $\text{dS}\cdot\text{m}^{-1}$  salinity,  $Chl_a$  was  $24.8 \pm 1.6 \mu\text{g}\cdot\text{cm}^{-2}$ , and at zero salinity level the content was  $16.9 \pm 1.1 \mu\text{g}\cdot\text{cm}^{-2}$ . Similarly, the higher total leaf chlorophyll contents ( $Chl_t$ ) were found in plants receiving a double dose of fertilizer, again with the maximum value of  $43.8 \pm 3.4 \mu\text{g}\cdot\text{cm}^{-2}$  observed at the highest salinity levels. With a decrease in the salinity level, the  $Chl_t$  decreased sharply to  $23.8 \pm 0.9 \mu\text{g}\cdot\text{cm}^{-2}$ . Although a decrease in salinity levels reduced the  $Chl_t$  at lower doses of fertilizer, the decrease was not as sharp as that of the double fertilizer dose.

Figure 1 presents the effect of both salinity and fertilizer on leaf pigments content per unit leaf area. As can be seen, the results indicate a significant increase in the content of all pigments with increasing salinity and fertilizer dose. However, the impact differs between the various pigments,

and is dependent on the combination of salinity-nutrient levels. Fertilizer dose increased the pigment content across all salinity levels, but the effect was most significant at mid-range salinity levels ( $7.0 \text{ dS}\cdot\text{m}^{-1}$ ). A doubling of the fertilizer dose at this medium salinity level resulted in an increase of over 200% in  $\text{Chl}_t$  per leaf area, compared to the zero fertilizer treatment (Supplementary Table S1).

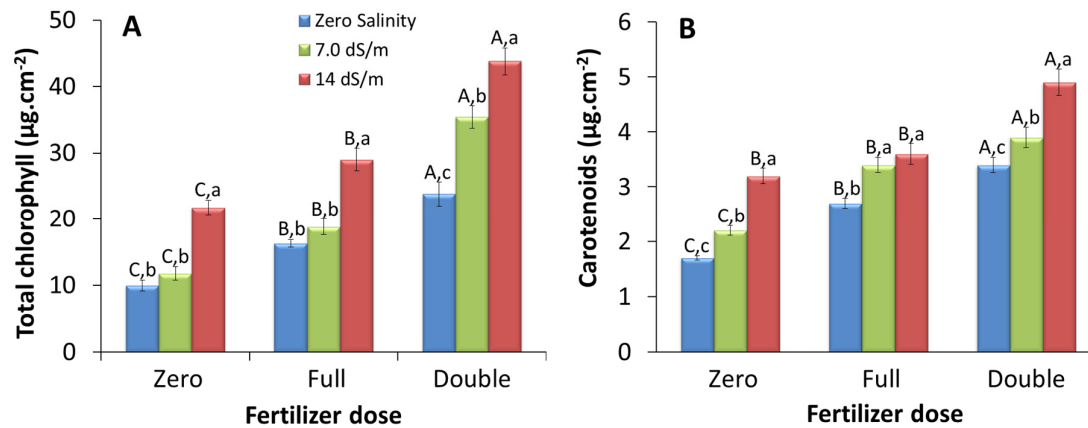


**Figure 1.** Pigment contents in wheat leaf under various treatments employed in the experiment expressed as  $\mu\text{g}\cdot\text{cm}^{-2}$ : (A) total chlorophyll and (B) total carotenoids content. Fertilizer treatments are grouped along the x-axis, and different color bars represent treatment of salinity. ANOVA was performed to test the effect of salinity and fertilizer treatments and their interaction. The post-hoc analysis was performed using Tukey's HSD test. Statistically significant differences are represented by different letters above the bars. Different capital letters indicate significant differences among the three fertilizer doses at a given salinity level (two-way ANOVA, Tukey's test,  $p < 0.01$ ). Different lowercase letters indicate significant differences among salinity treatments in each fertilizer dose (two-way ANOVA, Tukey's test,  $p < 0.01$ ). Means with same letters show non-significant difference at  $p < 0.01$ . Values are means of ~30 observations with error bars as standard deviations of the mean.

Statistical analysis showed that the effect of fertilizer dose on  $\text{Chl}_t$  was significant ( $p < 0.01$ ) at all salinity levels. On the other hand, the salinity levels showed a significant difference only at the double dose of fertilizer. For the zero and full fertilizer dose, only the highest salinity level was significantly different, with the zero and medium dose showing a non-significant difference. As noted earlier, plants grown under the double fertilizer dose produced the highest  $\text{Chl}_a$  content per leaf area at medium salinity levels, showing a 226% increase over plant leaves in the zero fertilizer treatment. The same fertilizer dose resulted in a 145% increase at the zero salinity and 103% increase at the highest salinity level of  $14 \text{ dS}\cdot\text{m}^{-1}$ .  $\text{Chl}_b$  content per leaf area exhibited similar treatment responses. Relative to zero fertilizer, a double dose of fertilizer caused a marked increase in  $\text{Chl}_b$  at zero (123%), medium (137%), and highest [37] levels of salinity. Correspondingly, the  $\text{Chl}_t$  content per leaf area showed a 200% increase at medium levels of salinity in response to the double dose relative to zero dose fertilizer application. At zero and high salinity levels, the corresponding change in  $\text{Chl}_t$  per leaf area was 138% and 101%, respectively (Table S1).

For  $\text{C}_t$  content, the impact of fertilizer was particularly pronounced in the absence of salinity, gradually declining with increases in salinity levels (Figure 1). For the  $14 \text{ dS}\cdot\text{m}^{-1}$  salinity level, there was a non-significant difference between zero and full fertilizer dose, while the double dose showed a statistically significant difference. A double dose of fertilizer relative to zero fertilizer increased the  $\text{C}_t$  content by 100% at zero salinity, 77% at  $7 \text{ dS}\cdot\text{m}^{-1}$ , and 53% at  $14 \text{ dS}\cdot\text{m}^{-1}$  salinity. In the case of  $\text{Chl}_t$ , the highest increment due to fertilizer appeared at the  $7 \text{ dS}\cdot\text{m}^{-1}$  salinity level. These results suggest that a doubling of fertilizer dosage is beneficial in increasing the pigment content at medium levels of salinity. However, further increases in salinity will diminish the beneficial effects of an increasing fertilizer dose (Figure 1B).

Plants grown under higher salinity treatments were characterized by considerably higher photosynthetic pigment content per leaf area across all fertilizer doses (Figure 1). However, the rates of increase in pigment content in response to increasing levels of salinity varied over the range of fertilizer application. The highest boost in the pigment content relative to the zero salinity treatment was observed at the 14 dS·m<sup>-1</sup> salinity level for the zero fertilizer applications (Supplementary Table S1). The resulting changes were 128%, 97%, 118%, and 88% for Chl<sub>a</sub>, Chl<sub>b</sub>, Chl<sub>t</sub>, and C<sub>t</sub> content, respectively. On the other hand, the highest increase in pigment content induced by fertilizer dose was observed at the medium (7 dS·m<sup>-1</sup>) salinity level. Interestingly, salinity-induced increases in pigment content were enhanced in the case of zero fertilizer applications. This supports the finding that salinity and fertilizer doses have an antagonistic effect on pigment content at high salinity levels in the growth media.

### 2.1.2. Whole Plant-Based Pigment Content

Any kind of biotic or abiotic stress is expected to challenge the overall health of vegetation. As has been observed, salinity stress tends to induce higher photosynthetic pigment content when expressed on a unit leaf area basis (Figure 1) for a specific fertilizer application. However, this tendency is reversed when expressing the pigment content on a per-plant basis (Figure 2) at the same fertilizer levels. While the effect of increasing fertilizer dose reflects the same increasing trend evident for the pigment content per unit leaf area, increasing soil salinity induces a decrease in the total amounts of leaf photosynthetic pigments. Increasing fertilizer dose significantly ( $p < 0.01$ ) enhanced Chl<sub>t</sub> and C<sub>t</sub> under each salinity treatment. On the contrary, all levels of salinity treatments significantly reduced the Chl<sub>t</sub> and C<sub>t</sub> at full and double fertilizer dose.

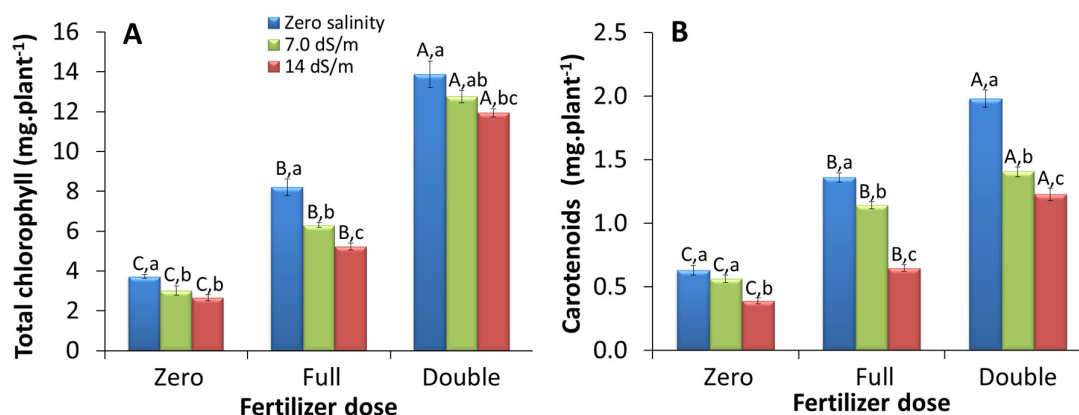


**Figure 2.** Actual amount of leaf pigments produced by a whole wheat plant under various treatments employed in the experiment expressed as mg·Plant<sup>-1</sup>: (A) total chlorophyll and (B) total carotenoids content. Fertilizer treatments are grouped along the x-axis and different color bars represent the salinity treatment. ANOVA was performed to test the effect of treatments of salinity and fertilizer and their interaction. The post-hoc analysis was performed using Tukey's HSD test. Statistically significant differences are presented by different letters above the bars. Different capital letters indicate significant differences among the three fertilizer doses at a given salinity level (two-way ANOVA, Tukey's test,  $p < 0.01$ ). Different lowercase letters indicate significant differences among salinity treatments in each fertilizer dose (two-way ANOVA, Tukey's test,  $p < 0.01$ ). Means with the same letters show non-significant difference at  $p < 0.01$ . Values are means of ~30 observations with error bars as standard deviations of the mean.

At the zero fertilizer dose, the difference between medium and high salinity treatments was non-significant. For all of the evaluated pigments, the fertilizer effect was particularly pronounced at the highest salinity treatment (14 dS·m<sup>-1</sup>), where the double dose fertilizer application increased Chl<sub>a</sub>, Chl<sub>b</sub>, Chl<sub>t</sub>, and C<sub>t</sub> contents by 354%, 342, 348%, and 214%, respectively (Table S1). Increasing salinity levels reduced the pigment content per plant across the entire range of applied fertilizer treatments.

For example, at the full fertilizer dose, relative changes of  $-55\%$  to  $-110\%$  in pigment content per plant occurred at the high relative to zero salinity treatment. These results reinforce the finding that higher amounts of fertilizer increase the detrimental effects of salinity on the photosynthetic pigments.

To further characterize the impact of these treatments on plant response, we examined the interrelationships between  $\text{Chl}_a$ ,  $\text{Chl}_b$ ,  $\text{Chl}_t$ , and  $C_t$  content across the different levels of salinity treatments. Not surprisingly,  $\text{Chl}_a$  and  $\text{Chl}_b$  were found to be closely associated with each other. Previous studies have also reported a close correspondence across the photosynthetic pigments, with  $\text{Chl}_a$  being 2 to 4 times higher than  $\text{Chl}_b$ , depending on the plant species, growth stage, and environmental conditions [85–87]. As shown in Figure 3A, the results from this study reflect a strong and positive linear relationship between  $\text{Chl}_a$  and  $\text{Chl}_b$  ( $R^2 = 0.95$  and  $\text{RMSE} = 2.71$ ), although a curvilinear tendency appears beyond a  $\text{Chl}_b$  value of around  $18 \mu\text{g}\cdot\text{cm}^{-2}$ . The ratio of  $\text{Chl}_a/\text{Chl}_b$  ranged from 0.73 to  $2.98 \mu\text{g}\cdot\text{cm}^{-2}$ , with an average value of  $2.47 \pm 0.38$  across the experiment. Although there was a tendency of an increasing ratio of  $\text{Chl}_a/\text{Chl}_b$  with increasing salinity level, the effect was not statistically significant. The  $C_t$  content was closely related to  $\text{Chl}_t$ . Figure 3B shows the relationship between  $\text{Chl}_t$  (i.e.,  $\text{Chl}_a + \text{Chl}_b$ ) and  $C_t$  content as described by a second-order power curve and using data obtained across all levels of salinity and fertilizer application. The curvilinear shape of the fitting function indicates a decreasing sensitivity of  $C_t$  content to changes in  $\text{Chl}_t$  with increasing  $\text{Chl}_t$ , before reaching an asymptotic level at  $\text{Chl}_t \sim 50 \mu\text{g}\cdot\text{cm}^{-2}$  (Figure 4A). Sims and Gamon [88] reported a similar relationship between  $\text{Chl}_t$  and  $C_t$  content across a wide range of plant species with variable leaf structure, plant functional type, and phenological development stage. In terms of salinity treatments, there is no clear trend in the impact of salinity gradients on the relationship between the plant pigments, although measurements taken from leaves exposed to zero salinity are centered more towards the lower extreme of the observed range (Figure 3B).

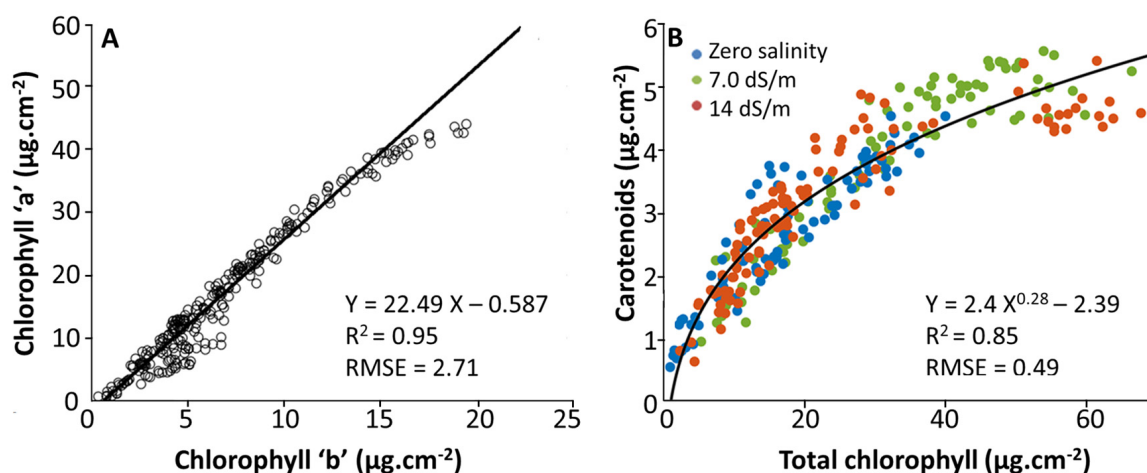


**Figure 3.** Relationship of the photosynthetic pigments in wheat leaves grown across gradients of soil salinity and fertilizer application: (A) linear relationship between chlorophyll “a” and chlorophyll “b” contents ( $n = 277$ ), and (B) relationship between total chlorophyll and carotenoids content ( $n = 277$ ) at various levels of salinity shown by different color markers. A second-order power curve best fitted to the data. The relationship coefficients and goodness of fit parameters are given in the plot area.

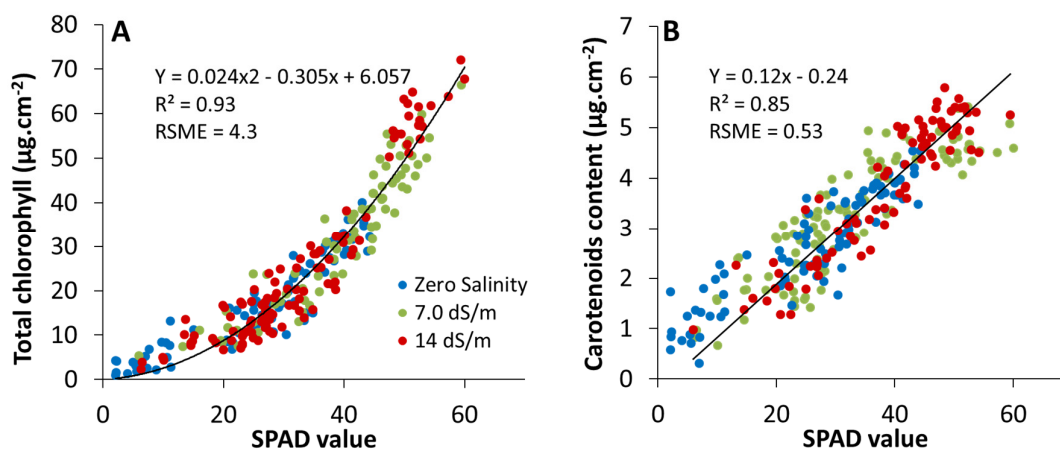


**Figure 4.** Relationships between SPAD-502 readings and the pigments at various levels of salinity and fertilizer application: (A) SPAD-502 vs. total chlorophyll content, and (B) SPAD-502 vs. total carotenoids content. Second-order polynomial curve was fitted to the data of total chlorophyll content, whereas a linear curve was fitted to the carotenoids data ( $n = 277$  in each case).

## 2.2. Estimation of Leaf Photosynthetic Pigment Content from SPAD-502 Measurements

SPAD readings ranged from 2.1 to 62.5 (unitless), and the highest value was found in plants grown under the double fertilizer dose in combination with the highest salinity level. Figure 4A shows the relationship between measurements of SPAD-502 and  $Chl_t$ , with values for all fertilizer treatments plotted at the defined salinity applications. A second-order polynomial provided the best approximation, yielding an overall  $R^2$  of 0.93 and RMSE of  $4.3 \mu\text{g}\cdot\text{cm}^{-2}$ . The relationship between leaf  $C_t$  content and SPAD readings was better described by a first-order linear equation, with an  $R^2$  of 0.85 and RMSE of  $0.53 \mu\text{g}\cdot\text{cm}^{-2}$  (Figure 4B). These regression models originate from a sufficiently large SPAD-pigments data set ( $n = 277$ ) that encompasses a broad range of leaf measurements taken from plants grown under salinity levels from 0–14  $\text{dS}\cdot\text{m}^{-1}$  and from zero fertilizer to double the dose of fertilizer recommended for wheat. As a result, derived expressions may be effectively used in a variety of field situations to calculate leaf photosynthetic pigment content from SPAD-502 readings. However, as the data come from different plants under different treatments (Figure 4), it is worthwhile to further diagnose the underlying structure and variation of the data resulting from different salinity treatment levels.

For this purpose, we examined whether the predictive power of salinity-specific regression models differed significantly. Accordingly, test procedures were performed to (1) explore cluster analysis to show how data pairs from different salinity treatments are grouped; (2) evaluate the statistical difference between the Pearson correlations ( $R$  values) of SPAD-chlorophyll and SPAD-carotenoids relationship obtained from the paired data at the three salinity levels; and (3) determine if the predictions based on the salinity-specific models deviate significantly from the overall regression model.

### 2.2.1. Cluster Analysis between SPAD and Pigment Content Values

Cluster analysis groups similar data into clusters and allows the specification of inter-cluster relationship to be determined. The SPAD readings and pigment data pairs for each measurement point were plotted, and an ellipse of  $2\sigma$  covariance was drawn around the mean point of each cluster. The ellipse dimensions are generated by the eigenvalues of the covariance matrix, with the biggest eigenvector alongside the main axis. Figure 5 displays the cluster analysis of the relationship between SPAD-502 readings and  $Chl_t$  and  $C_t$  content. As illustrated in Section 3.1, a higher salinity and fertilizer dose increases the values of  $Chl_t$  and  $C_t$  content, and the same tendency is reflected in the SPAD readings. Therefore, data from the zero salinity treatment are clustered closest to the origin of the plot, whereas data from medium and high salinity treatments are clustered at progressively higher limits of

the axis. The response of the medium salinity treatment is almost entirely encompassed within the response of the zero salinity treatment, while being significantly different from the response of the high salinity treatment (Figure 5A). Although the means of the zero salinity and medium salinity treatments are very close to each other, the ellipse of the zero salinity data is larger, due to a larger range in the SPAD and pigment values under the zero salinity treatment. The largest clusters are generated for the high salinity treatment, which is characterized by the highest SPAD and photosynthetic pigment content values. However, the characteristics of individual clusters are not significantly different for both  $\text{Chl}_t$  and  $\text{C}_t$  content (Figure 5A,B).

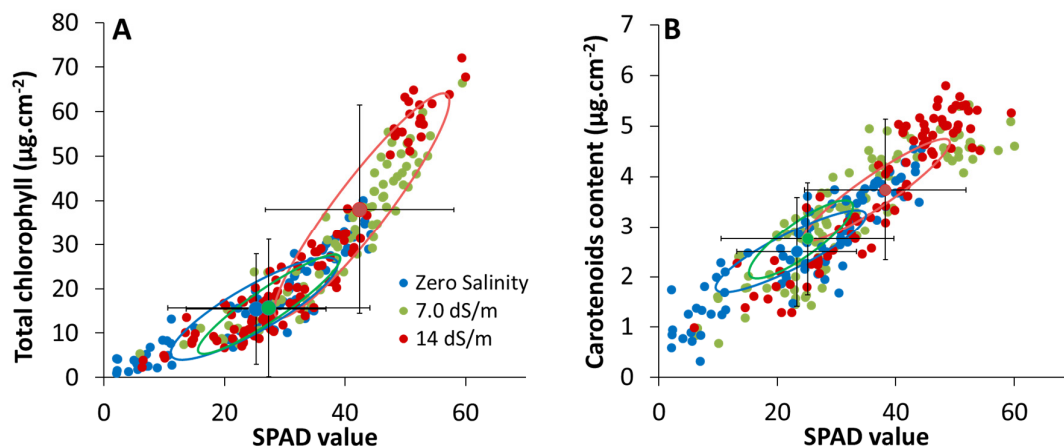


**Figure 5.** Cluster analysis of the relationships between SPAD-502 reading and the pigments at various levels of salinity and fertilizer application. (A) SPAD vs. total chlorophyll, (B) SPAD vs. total carotenoids content. The ellipses are calculated from the covariance matrix of the relationships. Whisker plots are superimposed on the data to illustrate the data spread ( $n = 277$ ).

### 2.2.2. Multivariate Statistical Analysis between SPAD and Pigment Content Values

The effect of salinity on the prediction of  $\text{Chl}_t$  content from the SPAD readings was also investigated based on a multivariate statistical analysis. This was performed to determine if salinity-specific regression models generated from the data at three different salinity levels were significantly different. The resulting Pearson correlations were 0.95, 0.95, and 0.97 for zero salinity, medium, and high salinity levels, respectively, indicating very strong and statistically significant ( $p < 0.001$ ) correlations. When the  $\text{Chl}_t$  values estimated through salinity-specific SPAD- $\text{Chl}_t$  regression models were plotted against those obtained from the overall regression model, they produced nearly overlapping lines, except for a small overestimation at the highest salinity level (Supplementary Figure S2A). This implies that the effect of fertilizer on the prediction of  $\text{Chl}_t$  per unit leaf area is the same at all levels of salinity stress, and that the more general regression model can describe most of the variability produced by any of the salinity-specific models. Similarly,  $\text{C}_t$  content estimated from an overall SPAD- $\text{C}_t$  regression model reproduced the overlapping lines when plotted against those estimated from salinity-specific regression models with an RMSE of  $0.53 \mu\text{g}\cdot\text{cm}^{-2}$ . However, at higher salinity levels, the overall SPAD- $\text{C}_t$  model is seen to slightly overestimate values at the lower range while slightly underestimating values at the higher range (Supplementary Figure S2B).

## 3. Discussion

Chlorophylls and carotenoids are key components of the photosynthetic machinery, and their role in harvesting light energy, stabilization of membranes, and energy transduction has been studied extensively [89–94]. SPAD measurements are widely used to assess the absolute chlorophyll content per leaf area in research settings and agricultural systems. In both instances, the effects of various abiotic factors on the estimation of these important plant traits require more detailed investigation.

Importantly, the link between SPAD measurement and photosynthetic pigments other than chlorophyll remains largely unexplored. In this work, we investigated the influence of salinity and nutrient stress and their interaction on  $\text{Chl}_t$  and  $\text{C}_t$  content on a per leaf and plant basis, combined with SPAD-502 readings of wheat at flowering stage, and determined the nature of SPAD–pigment relationships across large gradients in salinity and fertilizer treatment.

### 3.1. Effect of Stress on Pigment Content Per Unit Leaf Area

We observed that plants under increasingly saline treatments exhibited more green leaves compared to non-saline conditions. However, the overall size and volume of the green biomass was lower for the saline treatments. To partly offset the effects of stress, salinity usually results in thicker leaves with a higher number of cells per unit area, as well as decreased cell size in plant leaves [95,96]. The increased pigment per leaf area has previously been attributed to decreasing leaf growth in response to salinity stress [97]. Pandolfi et al. [98] suggested that stress may trigger a set of physiological alterations enabling the plants to withstand severe salinity. As was observed in our results, salinity stress tended to enhance the  $\text{Chl}_t$  and  $\text{C}_t$  content per leaf area (Figure 1), although the total pigment content per plant decreased as a result of smaller leaves. Previous studies have also shown that salinity stress increases  $\text{Chl}_t$  per leaf area in salt-tolerant plants [99], and an increase in  $\text{Chl}_t$  under salt stress could be used as a biochemical indicator of salt tolerance in plants [94,100]. Moderate salinity stress enhances the biosynthesis of  $\text{Chl}_t$  and  $\text{C}_t$  content in order to preserve proper functioning of the photosynthesis system. In that regard, our results are in agreement with Jiang et al. [94], who found that treatments with saline water significantly increased the leaf weight per area, along with  $\text{Chl}_t$  and  $\text{C}_t$  content, albeit for leaves of tomato plants. Similarly, Khatkar and Kuhad [101] correlated observed increases in  $\text{Chl}_t$  per leaf area to incremental increases in salinities (i.e., 5, 10, and 15  $\text{dS}\cdot\text{m}^{-1}$ ) in their study on wheat cultivars at the flowering stage.

Limited nutrient supply resulted in decreased pigment content per unit area, as well as in the total amount produced per plant. The response to salinity stress was somewhat different, with increased salinity tending to increase pigment content. A variable response of chlorophyll content to salt stress has been reported for a range of species, depending on their level of salt tolerance [56,100,102,103]. As a defense mechanism in response to salinity stress, leaf thickness and mass per unit area increase, and thus specific leaf area (SLA) can decrease. Visual observations of the plants during the experiment showed a pattern of deeper green color combined with thicker and narrower leaves. However, the total leaf mass and pigment amount produced per plant decreased with increasing salinity stress. Stress has varying effects on SLA. In typical cases [81,100,103], SLA has shown decreased values under drought/salinity stress as an adaptation to the prevailing stress. A logical explanation is that the lower surface area per leaf mass would result in less transpiration and conservation of water. Marron et al. [104] reported that a low SLA enhances the conservation of acquired resources, due to their higher dry matter content, thicker cell walls, and elevated concentration of secondary metabolites for prolonged survival of leaves.

### 3.2. Total Amount of Pigments Produced Per Plant

The interaction effect of salinity and fertilizer on the pigment content per leaf area was found to be significant, with a dependence of the salinity effect on the level of fertilizer application (Figures 1 and 2). Compared to the control (i.e., non-saline conditions with no fertilizer applied), the largest increase in  $\text{Chl}_t$  per leaf area was reported in leaves exposed to the highest salinity stress in combination with a double dose of fertilizer. This suggests that fertilizer can be utilized more effectively at higher levels of salinity. High concentrations of salts in the root zone cause imbalances in nutrient supply to the plant [97,105,106] by competitive interaction of the salts with nutrient ions or by membrane selectivity for the ions [51]. Moreover, plants under salinity stress produce more stress proteins, prolines, and compatible osmolytes [107–109]. Thus, being an integral component of the structures and functions, an optimum supply of essential plant nutrients is required for biochemical reactions

and synthesis of the biomolecules in stressful environments. These factors may provide an explanation for the observed response of pigment content to fertilizer at higher salinity levels.

### 3.3. Effect of Stress on SPAD–Pigment Relationships

To date, relatively few studies have assessed the effect of abiotic stress factors on SPAD–pigment relationships. A strong and highly significant correlation was established between SPAD-502 readings and  $\text{Chl}_t$  ( $R^2 = 0.93$ ) by fitting a second-order polynomial to the data (Figure 4A). Previous studies have shown that the relationship is plant-specific to some extent [80,110–112], and depending on the data, a variety of fitting models have been used to describe the relationship. Campbell et al. [113] found that linear models of SPAD–chlorophyll relationships differed between experiments and environmental conditions. Houborg et al. [114] fit an exponential model to the relationship between SPAD readings and dimethylsulfoxide (DMSO) extractable  $\text{Chl}_t$  per leaf area. Our study found a linear relationship between SPAD-502 and  $\text{C}_t$  content per leaf area when data was pooled from various treatments (Figure 4B). Similar relationships have been demonstrated with variable strengths of the coefficients [63,64,115]. It is clear from Figure 4B that indirect quantification of the  $\text{C}_t$  content is possible from SPAD-502 readings over the whole range of measurement. This finding differs somewhat from results reported in Netto et al. [77] in their study on coffee plants, which found a weak polynomial relationship below SPAD readings of 25. To better understand the utility of a generalized relationship, we further investigated the impact of salinity stress on the nature of the fitted models (Supplementary Figure S1). High Pearson correlations indicated strong and statistically significant ( $p < 0.001$ ) correlations at all levels of salinity. The correlation coefficients were not significantly different under various levels of salinity, and the overall regression model only slightly overestimated  $\text{Chl}_t$  at the highest salinity compared to the salinity-specific regression models. Likewise,  $\text{C}_t$  content estimated from the overall regression model only differed slightly from those estimated from salinity-specific regression models, with the largest deviations occurring during the high salinity treatment. As a result, for the particular wheat variety examined here, distinctive models developed at specific plant stress levels are not required to optimize predictability across different levels of salinity.

While the salinity-induced variations in the prediction models were found to be statistically non-significant, the small differences that were observed may be attributed to alterations in the internal structure of the leaf caused by saline conditions in the root zone. For instance, at a certain value of  $\text{Chl}_t$ , the corresponding SPAD value may differ due to internal leaf structural changes caused by salinity. SPAD-502 recordings are based on measurements of leaf transmittance at 650 nm and 940 nm [80]. Leaf spectral properties are governed by two distinct features of plant leaves. One is the biochemical composition of the leaf tissues, which include the plant photosynthetic pigments, biomolecules, and osmolytes. The other is the morphology and internal architecture of the leaf. The spectral response in the near-infrared region is affected by internal leaf structure [116]. Thus, even if the pigment content remains unchanged, alteration in micromorphology due to salinity stress may translate into variation in the spectral properties. Therefore, it is possible to have the same extractable chlorophyll content for two leaves showing quite different SPAD measurement values under changing and stressed environmental conditions. Studies have shown that due to high salt concentrations in the root zone, plant leaf micro-morphological and ultra-structural features are strongly altered in both halophytes and glycophytes [117,118]. A variable instrumental response to chlorophyll content has also been reported by Kalaji et al. [119] under nutrient-deficient conditions. The ultra-structural alterations may be caused by specific ion toxicity and osmotic imbalance [120]. The swelling of thylakoids in chloroplast may be induced by an osmotic imbalance between stroma and cytoplasm [117,121], which can result in photochemical oxidation. Vacuolation is another adaptive response to accumulate excess Na [122]. These leaf anatomical modifications may alter the spectral response and SPAD readings accordingly. However, in this specific study, the changes found in the regression coefficients of the fitted models did not vary significantly.

## 4. Materials and Methods

### 4.1. Greenhouse Pot Experiment

A greenhouse-based pot experiment was undertaken within an automated day–night temperature-controlled environment. For accuracy, a two-fold environmental monitoring system was installed that comprised of: (1) a data-logger connected with a Vaisala HMP155 for measuring ambient air temperature and relative humidity within the greenhouse; and (2) five Thermachron iButtons placed in close proximity to the growing plants, also to monitor temperature and relative humidity. Throughout the experiments, the temperature in the greenhouses was set to 25 °C during the day and 20 °C at night. The growing medium was a mixture of mineral soil collected from a nearby field and commercial organic soil. The field soil is classified as a calcareous alluvium Aridisol (Typic Haplargid), which is a coarse-loamy textured, thermic, and nutrient-deficient soil [123]. The field-collected soil was air-dried, ground, and passed through a 2-mm sieve. The mineral soil was amended with a commercial organic soil-mix with a ratio of 70:30 (*v/v*) and placed into 2.5 L plastic pots, ensuring a bulk density of 1.2 g·cm<sup>-3</sup> (typical of a plow layer in a cultivated field). The total amount of soil in each pot was measured on a dry weight basis, hence the water content of the soil needed to be known. To do this, the gravimetric water content ( $\theta_d$ ) of both the mineral soil and organic soil-mix was determined prior to mixing in order to establish the amount of soil required to fill the pots:

$$\theta_d = \frac{W_{wet} - W_{dry}}{W_{dry}} \quad (1)$$

where  $W_{wet}$  is weight of wet soil and  $W_{dry}$  is weight of oven-dry soil. The water holding capacity (WHC) of the soil was determined by the amount of water retained by the saturated soil after free drainage for two days according to:

$$\text{WHC (\%)} = \frac{\text{weight of drained soil} - \text{weight of air dried soil}}{\text{weight of air dried soil}} \times 100 \quad (2)$$

Plants were grown at a WHC of nearly 70% during the experimental period through a regulated irrigation in which water lost from a pot via evapotranspiration was replenished with fresh non-saline irrigation water. The water lost was measured as the difference between weights of each pot between two irrigation time intervals.

Spring wheat (*Triticum aestivum* L., Australian Grain Technologies MACE variety) was used as the primary plant material during the experiment. Four seeds were sown in each pot. On the tenth day after sowing, over 90% germination was observed. The pots were then thinned to two uniformly germinated plants per pot for the remainder of the experiment.

#### 4.1.1. Plant Treatments

A total of nine treatments, each with three replicates (27 experimental units), were employed in the experiment using a randomized complete block design. Blocks were assigned with different soil salinity treatments, and the fertilizer treatments were randomized within each block of salinity. Non-saline irrigation water was applied once a week during the early growth stages and then twice weekly after booting stage, as water loss was greater during this stage of vegetation growth. The soil was salinized by saturating selected pots with specified salinities of irrigation water ( $S_1 = 0.3$ ,  $S_2 = 7.0$ , and  $S_3 = 14$  dS·m<sup>-1</sup>). The electrical conductivity (EC) levels of the applied water were selected according to observed plant responses to salinity during a preliminary experiment. During that experiment, salinity levels were chosen according to salinity tolerances of wheat as reported by FAO irrigation water quality criteria [124]. The salinity levels were obtained by mixing tap water (desalinated seawater) with fresh sea water (EC = 59.8 dS·m<sup>-1</sup>) under continuous stirring and monitoring of the EC during mixing.

In addition to salinity treatment, three levels of fertilizer (F1, F2, F3) were employed during the experiment to represent zero, full, and double dose of that recommended for wheat (Figure 6). Slow-release granular fertilizer (commercially available MIKAFOZ<sup>®</sup>, Agriculture Machinery & Materials Co. Ltd., Jeddah, Saudi Arabia) blended with micronutrients (18-18-5 + TE; i.e., 18% nitrogen, 18% phosphorous, 5% potassium, and trace elements) was applied at 3 cm depth in each pot. The amount of fertilizer required for each pot was calculated based on the soil surface area of the pot. Given the radius ( $r$ ) of the pot (7.3 cm), surface area ( $A$ ) was measured as  $A = \pi r^2$ . The full dose of fertilizer was considered as  $120 \text{ kg}\cdot\text{N}\cdot\text{ha}^{-1}$  recommended for wheat crop.

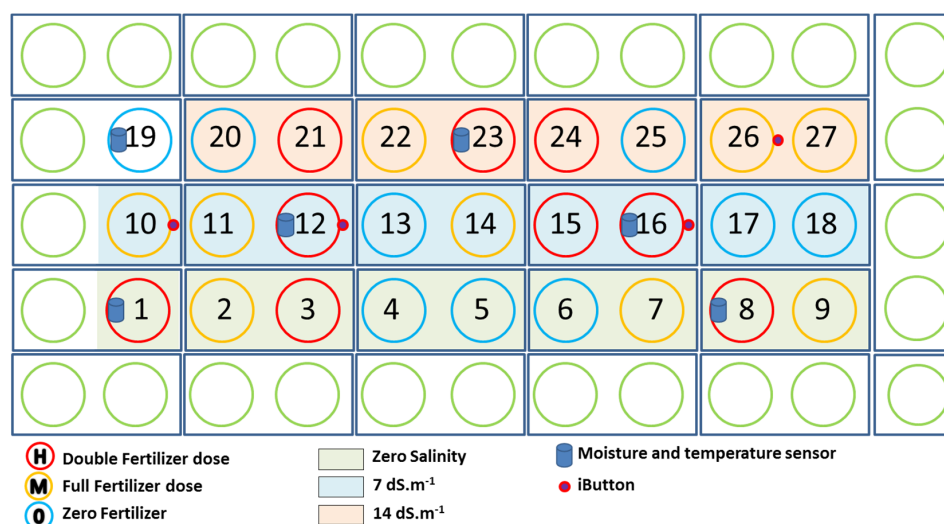


**Figure 6.** Experimental setup showing the arrangement of the applied treatments as well as the sensors used for environmental monitoring. Each numbered circle represents a pot containing two plants. Salinity and fertilizer treatments were applied in a randomized complete block design with three replications. Blocks (colored rows) were assigned a fixed salinity, while fertilizer treatments in three replications were randomized within each row. Green circles represent buffer pots containing plants without treatment encircling the treatment pots. Blue circles are pots with no fertilizer, yellow circles are pots receiving full fertilizer dose and red circles show double the recommended fertilizer dose.

Measurements and sample collection for determination of  $\text{Chl}_a$ ,  $\text{Chl}_b$  [57],  $\text{Chl}_t$ , and  $C_t$  content were undertaken within 2 days at the anthesis stage. This period is known as the lag phase, during which cellular division is rapid and endosperm cells and amyloplasts are formed, and is considered very sensitive to environmental stresses [125].

#### 4.1.2. SPAD Measurements

The SPAD-502 meter is used extensively in research and agricultural settings as a rapid, inexpensive, and non-destructive method for the assessment of leaf chlorophyll content. The SPAD-502 meter consists of two light-emitting diodes (LEDs) and a silicon photodiode receptor. It measures leaf transmittance in the red region (650 nm) and infrared region (940 nm) of the electromagnetic spectrum. A relative SPAD-502 meter value (ranging from 0–99) is derived from the transmittance values, which is proportional to the chlorophyll content in the sample [75,80].

From each plant, 10 leaves of varying age and color were selected for measurements made under diffuse lighting [84]. Every leaf measurement was an average of 10–15 SPAD-502 readings.

#### 4.2. Photosynthetic Pigments Determination

Leaf chlorophyll and  $C_t$  contents were determined by spectrophotometric analysis of chemically extracted pigments. For this purpose, a total of 270 samples [87] were collected immediately after

the SPAD-502 measurements across the prescribed gradients of soil salinity and fertilizer treatment. For each of these samples, three leaf discs with a diameter of 7 mm (area = 0.38 cm<sup>2</sup>) were collected in a micro-centrifuge Eppendorf tube, and immediately wrapped in aluminum foil and stored in ice. The samples were transported within 30 min of collection to the laboratory and stored at −80 °C until final analysis could be undertaken using the methods of Arnon [126] and Wellburn [115]. Briefly, the samples were ground in liquid nitrogen using the SPEX Sample Prep™ CryoStation (2600) and Geno/Grinder. The ground samples were extracted in 80% ethanol at room temperature after centrifugation. Pigment absorption was measured spectrophotometrically at 663, 645, and 470 nm using an Infinite M1000 PRO plate reader, and translated into pigment contents using the following equations:

$$\text{Chl}_t \left( \mu\text{g}\cdot\text{cm}^{-2} \right) = [(20.2 \times A_{645}) + (8.02 \times A_{663})] \times \text{mL of Acetone}_{80\%} / \text{Leaf Area} \left( \text{cm}^2 \right) \quad (3)$$

$$\text{Chl}_a \left( \mu\text{g}\cdot\text{cm}^{-2} \right) = [(12.7 \times A_{663}) - (2.6 \times A_{645})] \times \text{mL of Acetone}_{80\%} / \text{Leaf Area} \left( \text{cm}^2 \right) \quad (4)$$

$$\text{Chl}_b \left( \mu\text{g}\cdot\text{cm}^{-2} \right) = [(22.9 \times A_{645}) - (4.68 \times A_{663})] \times \text{mL of Acetone}_{80\%} / \text{Leaf Area} \left( \text{cm}^2 \right) \quad (5)$$

$$C_t \left( \mu\text{g}\cdot\text{cm}^{-2} \right) = [(1000 \times A_{470}) - (1.9 \times \text{Chl}_a) - (63.14 \times \text{Chl}_b)] / 214 \quad (6)$$

where A is absorbance at the subscript wavelength. The total pigment content produced per plant,  $P_p$  (mg·plant<sup>−1</sup>), was calculated from the pigment content per leaf area ( $P_L$ ) and the total leaf area per plant ( $A_p$ ) as:

$$P_p = P_L \times A_p \quad (7)$$

A subset of leaf samples was collected from each salinity treatment for the measurement of leaf area using a portable leaf area meter (LI-3000C, Li-COR Inc., Lincoln, NE, USA) and a connected conveyer belt (LI-3050C, LI-COR Inc.). The leaf material for each treatment was dried in an oven for 2 days at 60 °C and weighed in order to calculate the specific leaf area for each salinity treatment. The  $A_p$  for all individual plants was then calculated by multiplying the specific leaf area with the total dry leaf weight of the plant [127].

#### 4.3. Statistical Analyses

Analyses of variance (ANOVA) of the means of the different treatments were performed in MATLAB (MathWorks, Natick, MA, USA) using two-way ANOVA analysis (ANOVA2). Tukey's honestly significance difference (HSD) test [128] was implemented using R-code to determine if the means were significantly different from each other:

$$\text{HSD} = \frac{M_1 - M_2}{\sqrt{\text{MS}_w \left( \frac{1}{n} \right)}} \quad (8)$$

where  $M_1$  and  $M_2$  denote the means of the two treatments being compared,  $\text{MS}_w$  is the mean square within the treatments (residual mean square), and  $n$  is number of observations in the treatment.

For any particular salinity level (denoted in Figures 1 and 2 by one of three colors), a different capitalized letter across the varying fertilizer doses (i.e., zero, full, and double) indicates a statistically significant difference. Differing lowercase letters placed on the three color bars within any fertilizer dosage indicates a significant difference between the particular salinity treatments. For cases having the same letters on individual bars, either across dosages or salinity levels, the differences are statistically non-significant. For example, in Figure 1A, we see that the red bars each have a different capital letter, indicating that the results across fertilizer doses is statistically significant at that particular salinity level (14 dS·m<sup>−1</sup>). On the other hand, in Figure 1B at 14 dS·m<sup>−1</sup>, there is a non-significant difference between zero and full fertilizer dose, but the double dose does show a statistically significant difference. Similarly, in Figure 1A, different lowercase letters placed on the three color bars within the double

fertilizer dose indicate significant differences among the salinity treatments in that group. However, for the zero and full fertilizer dose, only the red bar (14 dS·m<sup>-1</sup>) salinity level is significantly different. Further, the mutual differences of blue and green bars are non-significant for these particular cases.

Regression analysis was performed using SPSS Version 10.0 [129]. After fitting suitable regression models to the pigment data, RMSE (root mean square error) was calculated as follows:

$$RMSE = \sqrt{\frac{1}{N} \sum_{i=1}^N (Y_i - \hat{Y}_i)^2} \quad (9)$$

where  $N$  denotes the number of observations,  $Y_i$  is the measured value, and  $\hat{Y}_i$  is the estimated value of the dependent variable. Cluster analyses on the scatter plots were performed to further characterize the variability of the derived relationships. This statistical technique is commonly used in data mining and exploratory analysis to group data based on similarities called clusters, helping to describe the relationship of the clusters to each other and to the independent variable. In this technique, data pairs of independent and dependent variables for each point of measurement are plotted. For each cluster of data, an ellipse of  $2\sigma$  covariance is described around the mean point of the cluster. The dimensions of the ellipse are the eigenvalues of the covariance matrix that is revolved in a way to ensure that the main axis lies alongside the largest eigenvector.

## 5. Conclusions

Wheat plants under salinity stress showed a significant increase in the chlorophyll and  $C_t$  content per leaf area, whereas salinity stress significantly reduced leaf dry matter and total content of the produced pigments when accounting for pragmatic changes in leaf area. Although fertilizer applications enhanced the photosynthetic pigment content per leaf area, their interaction with salinity stress was found to be significant and varied with the level of salinity present in the root zone. Unlike the pigment content per unit area, the total amount of pigment content per plant was significantly reduced by the imposed salinity stress. In terms of monitoring the  $Chl_t$  and  $C_t$  content of the plant in a passive and non-destructive manner, a strong positive and statistically significant correlation was found with SPAD-502 readings, based on a large experimental data set. The analyses indicated that the strength of the correlations remained largely unaffected by salinity stress and that the relatively small variations in model coefficients were the result of biochemical and structural alterations in leaves modified by the salinity stress. The results confirm that SPAD-based retrieval of photosynthetic pigments can be undertaken with some degree of confidence without considering specific conditions induced by prevailing stress in wheat plants.

**Supplementary Materials:** The following are available online at [www.mdpi.com/2073-4395/7/3/61/s1](http://www.mdpi.com/2073-4395/7/3/61/s1). Figure S1. Relationship between SPAD and chlorophyll content at various salinity levels. Figure S2. Difference between overall and salinity specific prediction models. Table S1. Variation in pigment content (%) under various treatment combinations.

**Acknowledgments:** The authors would like to extend their sincere appreciation to staff of the greenhouse, along with Prof Mark Tester and his Salt Laboratory (<https://saltlab.kaust.edu.sa>) for their support and access to facilities during the experimental period. Research reported in this publication was supported by the King Abdullah University of Science and Technology (KAUST).

**Author Contributions:** Experiments were designed by Syed Haleem Shah, Rasmus Houborg, and Matthew McCabe, Syed Haleem Shah performed the experiments, analyzed the data and wrote the initial draft of the manuscript. Rasmus Houborg and Matthew McCabe edited the manuscript.

**Conflicts of Interest:** The authors declare no conflict of interest.

## References

1. Blackburn, G.A. Hyperspectral remote sensing of plant pigments. *J. Exp. Bot.* **2007**, *58*, 855–867. [[CrossRef](#)] [[PubMed](#)]

2. Cannella, D.; Möllers, K.B.; Frigaard, N.U.; Jensen, P.E.; Bjerrum, M.J.; Johansen, K.S.; Felby, C. Light-driven oxidation of polysaccharides by photosynthetic pigments and a metalloenzyme. *Nat. Commun.* **2016**, *7*, 11134. [[CrossRef](#)] [[PubMed](#)]
3. Feret, J.-B.; François, C.; Asner, G.P.; Gitelson, A.A.; Martin, R.E.; Bidel, L.P.R.; Ustin, S.L.; le Maire, G.; Jacquemoud, S. Prospect-4 and 5: Advances in the leaf optical properties model separating photosynthetic pigments. *Remote Sens. Environ.* **2008**, *112*, 3030–3043. [[CrossRef](#)]
4. Huang, C.J.; Wei, G.; Jie, Y.C.; Xu, J.J.; Zhao, S.Y.; Wang, L.C.; Anjum, S.A. Responses of gas exchange, chlorophyll synthesis and ROS-scavenging systems to salinity stress in two ramie (*boehmeria nivea* L.) cultivars. *Photosynthetica* **2015**, *53*, 455–463. [[CrossRef](#)]
5. Zhao, D.; Reddy, K.R.; Kakani, V.; Read, J.; Carter, G. Corn (*Zea mays* L.) growth, leaf pigment concentration, photosynthesis and leaf hyperspectral reflectance properties as affected by nitrogen supply. *Plant Soil* **2003**, *257*, 205–218. [[CrossRef](#)]
6. Abramavicius, D.; Valkunas, L. Role of coherent vibrations in energy transfer and conversion in photosynthetic pigment-protein complexes. *Photosynth. Res.* **2016**, *127*, 33–47. [[CrossRef](#)] [[PubMed](#)]
7. Baťjuka, A.; Škute, N.; Petjukevičs, A. The influence of antimycin A on pigment composition and functional activity of photosynthetic apparatus of *triticum aestivum* L. Under high temperature. *Photosynthetica* **2016**, *55*, 1–14. [[CrossRef](#)]
8. Kocks, P.; Ross, J.; Björkman, O. Thermodynamic efficiency and resonance of photosynthesis in a C3 plant. *J. Phys. Chem.* **1995**, *99*, 16483–16489. [[CrossRef](#)]
9. Houborg, R.; McCabe, M.; Cescatti, A.; Gao, F.; Schull, M.; Gitelson, A. Joint leaf chlorophyll content and leaf area index retrieval from landsat data using a regularized model inversion system (regflec). *Remote Sens. Environ.* **2015**, *159*, 203–221. [[CrossRef](#)]
10. Gitelson, A.A.; Keydan, G.P.; Merzlyak, M.N. Three-band model for noninvasive estimation of chlorophyll, carotenoids, and anthocyanin contents in higher plant leaves. *Geophys. Res. Lett.* **2006**, *33*, L11402. [[CrossRef](#)]
11. Carter, G.A. Ratios of leaf reflectances in narrow wavebands as indicators of plant stress. *Int. J. Remote Sens.* **1994**, *15*, 697–703. [[CrossRef](#)]
12. Boegh, E.; Soegaard, H.; Broge, N.; Hasager, C.B.; Jensen, N.O.; Schelde, K.; Thomsen, A. Airborne multispectral data for quantifying leaf area index, nitrogen concentration, and photosynthetic efficiency in agriculture. *Remote Sens. Environ.* **2002**, *81*, 179–193. [[CrossRef](#)]
13. Sanglard, L.M.; Martins, S.C.; Detmann, K.C.; Silva, P.E.; Lavinsky, A.O.; Silva, M.M.; Detmann, E.; Araujo, W.L.; DaMatta, F.M. Silicon nutrition alleviates the negative impacts of arsenic on the photosynthetic apparatus of rice leaves: An analysis of the key limitations of photosynthesis. *Physiol. Plant* **2014**, *152*, 355–366. [[CrossRef](#)] [[PubMed](#)]
14. Holt, N.E.; Zigmantas, D.; Valkunas, L.; Li, X.P.; Niyogi, K.K.; Fleming, G.R. Carotenoid cation formation and the regulation of photosynthetic light harvesting. *Science* **2005**, *307*, 433–436. [[CrossRef](#)] [[PubMed](#)]
15. Zakar, T.; Laczko-Dobos, H.; Toth, T.N.; Gombos, Z. Carotenoids assist in cyanobacterial photosystem II assembly and function. *Front. Plant Sci.* **2016**, *7*, 295. [[CrossRef](#)] [[PubMed](#)]
16. Boo, Y.C.; Jung, J. Water deficit-induced oxidative stress and antioxidative defenses in rice plants. *J. Plant Physiol.* **1999**, *155*, 255–261.
17. Bouvier, F.; Isner, J.C.; Dogbo, O.; Camara, B. Oxidative tailoring of carotenoids: A prospect towards novel functions in plants. *Trends Plant Sci.* **2005**, *10*, 187–194. [[CrossRef](#)] [[PubMed](#)]
18. Campos, M.D.; Nogales, A.; Cardoso, H.G.; Campos, C.; Grzebelus, D.; Velada, I.; Arnholdt-Schmitt, B. Carrot plastid terminal oxidase gene (dcpTox) responds early to chilling and harbors intronic pre-miRNAs related to plant disease defense. *Plant Gene* **2016**, *7*, 21–25. [[CrossRef](#)]
19. Demmig-Adams, B.; Adams, W.W., III. The role of xanthophyll cycle carotenoids in the protection of photosynthesis. *Trends Plant Sci.* **1996**, *1*, 21–26. [[CrossRef](#)]
20. Santabarbara, S.; Casazza, A.P.; Ali, K.; Economou, C.K.; Wannathong, T.; Zito, F.; Redding, K.E.; Rappaport, F.; Purton, S. The requirement for carotenoids in the assembly and function of the photosynthetic complexes in *Chlamydomonas reinhardtii*. *Plant Physiol.* **2013**, *161*, 535–546. [[CrossRef](#)] [[PubMed](#)]
21. Nagy, L.; Kiss, V.; Brumfeld, V.; Osvay, K.; Börzsönyi, Á.; Magyar, M.; Szabó, T.; Dorogi, M.; Malkin, S. Thermal effects and structural changes of photosynthetic reaction centers characterized by wide frequency band hydrophone: Effects of carotenoids and terbutryn. *Photochem. Photobiol.* **2015**, *91*, 1368–1375. [[CrossRef](#)] [[PubMed](#)]

22. Flexas, J.; Bota, J.; Loreto, F.; Cornic, G.; Sharkey, T. Diffusive and metabolic limitations to photosynthesis under drought and salinity in C3 plants. *Plant Biol.* **2004**, *6*, 269–279. [[CrossRef](#)] [[PubMed](#)]
23. Chaves, M.M.; Flexas, J.; Pinheiro, C. Photosynthesis under drought and salt stress: Regulation mechanisms from whole plant to cell. *Ann. Bot.* **2009**, *103*, 551–560. [[CrossRef](#)] [[PubMed](#)]
24. Chuluun, B.; Shah, S.H.; Rhee, J.-S. Bioaugmented phytoremediation: A strategy for reclamation of diesel oil-contaminated soils. *Int. J. Agric. Biol.* **2014**, *16*, 624–628.
25. Lee, S.S.; Shah, H.S.; Awad, Y.M.; Kumar, S.; Ok, Y.S. Synergy effects of biochar and polyacrylamide on plants growth and soil erosion control. *Environ. Earth Sci.* **2015**, *74*, 2463–2473. [[CrossRef](#)]
26. Ashraf, M.; Harris, P.J.C. Photosynthesis under stressful environments: An overview. *Photosynthetica* **2013**, *51*, 163–190. [[CrossRef](#)]
27. Kato, M.; Shimizu, S. Chlorophyll metabolism in higher plants vi. Involvement of peroxidase in chlorophyll degradation. *Plant Cell Physiol.* **1985**, *26*, 1291–1301.
28. Oliveira, H.; Barros, A.S.; Delgadillo, I.; Coimbra, M.A.; Santos, C. Effects of fungus inoculation and salt stress on physiology and biochemistry of in vitro grapevines: Emphasis on sugar composition changes by ft-ir analyses. *Environ. Exp. Bot.* **2009**, *65*, 1–10. [[CrossRef](#)]
29. Filippou, P.; Antoniou, C.; Obata, T.; Van Der Kelen, K.; Harokopos, V.; Kanetis, L.; Aidinis, V.; Van Breusegem, F.; Fernie, A.R.; Fotopoulos, V. Kresoxim-methyl primes medicago truncatula plants against abiotic stress factors via altered reactive oxygen and nitrogen species signalling leading to downstream transcriptional and metabolic readjustment. *J. Exp. Bot.* **2016**, *67*, 1259–1274. [[CrossRef](#)] [[PubMed](#)]
30. Chen, J.B.; Yan, J.; Qian, Y.L.; Jiang, Y.Q.; Zhang, T.T.; Guo, H.L.; Guo, A.G.; Liu, J.X. Growth responses and ion regulation of four warm season turfgrasses to long-term salinity stress. *Sci. Hortic.* **2009**, *122*, 620–625. [[CrossRef](#)]
31. Wang, C.; Guo, Z.; Wang, S.; Wang, L.; Ma, C. Improving hyperspectral image classification method for fine land use assessment application using semisupervised machine learning. *J. Spectrosc.* **2015**, *2015*. [[CrossRef](#)]
32. Tester, M.; Bacic, A. Abiotic stress tolerance in grasses. From model plants to crop plants. *Plant Physiol.* **2005**, *137*, 791–793. [[CrossRef](#)] [[PubMed](#)]
33. Munns, R.; Tester, M. Mechanisms of salinity tolerance. In *Annual Review of Plant Biology*; Annual Reviews: Palo Alto, CA, USA, 2008; Volume 59, pp. 651–681.
34. Tester, M.; Davenport, R. Na<sup>+</sup> tolerance and Na<sup>+</sup> transport in higher plants. *Ann. Bot.* **2003**, *91*, 503–527. [[CrossRef](#)] [[PubMed](#)]
35. Poor, P.; Gemes, K.; Horvath, F.; Szepesi, A.; Simon, M.L.; Tari, I. Salicylic acid treatment via the rooting medium interferes with stomatal response, CO<sub>2</sub> fixation rate and carbohydrate metabolism in tomato, and decreases harmful effects of subsequent salt stress. *Plant Biol.* **2011**, *13*, 105–114. [[CrossRef](#)] [[PubMed](#)]
36. Hu, Y.; Fromm, J.; Schmidhalter, U. Effect of salinity on tissue architecture in expanding wheat leaves. *Planta* **2005**, *220*, 838–848. [[CrossRef](#)] [[PubMed](#)]
37. Tang, L.; Ying, R.R.; Jiang, D.; Zeng, X.W.; Morel, J.L.; Tang, Y.T.; Qiu, R.L. Impaired leaf CO<sub>2</sub> diffusion mediates Cd-induced inhibition of photosynthesis in the Zn/Cd hyperaccumulator *Picris divaricata*. *Plant Physiol. Biochem.* **2013**, *73*, 70–76. [[CrossRef](#)] [[PubMed](#)]
38. Schertz, F.M. The quantitative determination of chlorophyll. *Plant Physiol.* **1928**, *3*, 323–334. [[CrossRef](#)] [[PubMed](#)]
39. Pearman, I.; Thomas, S.M.; Thorne, G.N. Effect of nitrogen fertilizer on photosynthesis of several varieties of winter wheat. *Ann. Bot.* **1979**, *43*, 613–621. [[CrossRef](#)]
40. Yong, J.W.H.; Ng, Y.F.; Tan, S.N.; Chew, A.Y.L. Effect of fertilizer application on photosynthesis and oil yield of *Jatropha curcas* L. *Photosynthetica* **2010**, *48*, 208–218. [[CrossRef](#)]
41. Cai, R.-G.; Zhang, M.; Yin, Y.-P.; Wang, P.; Zhang, T.-B.; Gu, F.; Dai, Z.-M.; Liang, T.-B.; Wu, Y.-H.; Wang, Z.-L. Photosynthetic characteristics and antioxidative metabolism of flag leaves in responses to nitrogen application during grain filling of field-grown wheat. *Agric. Sci. China* **2008**, *7*, 157–167. [[CrossRef](#)]
42. Hosseinzadeh, S.; Amiri, H.; Ismaili, A. Effect of vermicompost fertilizer on photosynthetic characteristics of chickpea (*Cicer arietinum* L.) under drought stress. *Photosynthetica* **2016**, *54*, 87–92. [[CrossRef](#)]
43. Zhang, L.; Shangguan, Z.; Mao, M.; Yu, G. Effects of long-term application of nitrogen fertilizer on leaf chlorophyll fluorescence of upland winter wheat. *Chin. J. Appl. Ecol.* **2003**, *14*, 695–698.
44. Esmaili, E.; Kapourchal, S.A.; Malakouti, M.J.; Homaeae, M. Interactive effect of salinity and two nitrogen fertilizers on growth and composition of sorghum. *Plant Soil Environ.* **2008**, *54*, 537–546.

45. Semiz, G.D.; Suarez, D.L.; Ünlükara, A.; Yurtseven, E. Interactive effects of salinity and n on pepper (*capsicum annuum* L.) yield, water use efficiency and root zone and drainage salinity. *J. Plant Nutr.* **2014**, *37*, 595–610. [[CrossRef](#)]
46. Soliman, M.; Kostandi, S.; Van Beusichem, M. Influence of sulfur and nitrogen fertilizer on the uptake of iron, manganese, and zinc by corn plants grown in calcareous soil. *Commun. Soil Sci. Plant Anal.* **1992**, *23*, 1289–1300. [[CrossRef](#)]
47. El-Siddig, K.; Ludders, P. Interactive effects of nitrogen nutrition and salinity on reproductive growth of apple trees. *Gartenbauwissenschaft* **1994**, *59*, 127–131.
48. Patel, R.M. Effects of watertable depth, irrigation water salinity, and fertilizer application on root zone salt buildup. *Can. Biosyst. Eng.* **2000**, *42*, 111–115.
49. Zipelevish, E.; Grinberge, A.; Amar, S.; Gilbo, Y.; Kafkafi, U. Eggplant dry matter composition fruit yield and quality as affected by phosphate and total salinity caused by potassium fertilizers in the irrigation solution. *J. Plant Nutr.* **2000**, *23*, 431–442. [[CrossRef](#)]
50. Dhanda, S.K.; Toky, O.P. Interaction of provenance (seed source), fertilizers and salinities in eucalyptus tereticornis and e. Camaldulensis grown in north-west india. *Range Manag. Agrofor.* **2010**, *31*, 120–124.
51. Grattan, S.; Grieve, C. Salinity–mineral nutrient relations in horticultural crops. *Sci. Hortic.* **1998**, *78*, 127–157. [[CrossRef](#)]
52. Huang, J.R.; Sun, J.Y.; Liao, H.J.; Liu, X.D. Detection of brown planthopper infestation based on spad and spectral data from rice under different rates of nitrogen fertilizer. *Precis. Agric.* **2015**, *16*, 148–163. [[CrossRef](#)]
53. Ibrahim, W.; Ahmed, I.M.; Chen, X.; Wu, F. Genotype-dependent alleviation effects of exogenous gsh on salinity stress in cotton is related to improvement in chlorophyll content, photosynthetic performance, and leaf/root ultrastructure. *Environ. Sci. Pollut. Res.* **2017**, *24*, 1–11. [[CrossRef](#)] [[PubMed](#)]
54. Khoshbakht, D.; Ramin, A.A.; Baninasab, B. Effects of sodium chloride stress on gas exchange, chlorophyll content and nutrient concentrations of nine citrus rootstocks. *Photosynthetica* **2015**, *53*, 241–249. [[CrossRef](#)]
55. Sanchez, R.A.; Hall, A.J.; Trapani, N.; de Hunau, R.C. Effects of water stress on the chlorophyll content, nitrogen level and photosynthesis of leaves of two maize genotypes. *Photosynth. Res.* **1983**, *4*, 35–47. [[CrossRef](#)] [[PubMed](#)]
56. Turan, M.A.; Katkat, V.; Taban, S. Variations in proline, chlorophyll and mineral elements contents of wheat plants grown under salinity stress. *J. Agron.* **2007**, *6*, 137–141.
57. Qiu, T.; Jiang, L.; Li, S.; Yang, Y. Small-scale habitat-specific variation and adaptive divergence of photosynthetic pigments in different alkali soils in reed identified by common garden and genetic tests. *Front. Plant Sci.* **2017**, *7*, 2016. [[CrossRef](#)] [[PubMed](#)]
58. Gomez, P.I.; Barriga, A.; Cifuentes, A.S.; Gonzalez, M.A. Effect of salinity on the quantity and quality of carotenoids accumulated by dunaliella salina (strain conc-007) and dunaliella bardawil (strain atcc 30861) chlorophyta. *Biol. Res.* **2003**, *36*, 185–192. [[CrossRef](#)] [[PubMed](#)]
59. Borghesi, E.; González-Miret, M.L.; Escudero-Gilete, M.L.; Malorgio, F.; Heredia, F.J.; Meléndez-Martínez, A.J. Effects of salinity stress on carotenoids, anthocyanins, and color of diverse tomato genotypes. *J. Agric. Food Chem.* **2011**, *59*, 11676–11682. [[CrossRef](#)] [[PubMed](#)]
60. Akram, N.A.; Ashraf, M. Pattern of accumulation of inorganic elements in sunflower (*helianthus annuus* L.) plants subjected to salt stress and exogenous application of 5-aminolevulinic acid. *Pak. J. Bot.* **2011**, *43*, 521–530.
61. Khan, A.L.; Hamayun, M.; Kim, Y.H.; Kang, S.M.; Lee, I.J. Ameliorative symbiosis of endophyte (*Penicillium funiculosum* LHL06) under salt stress elevated plant growth of *glycine max* L. *Plant Physiol. Biochem.* **2011**, *49*, 852–861. [[CrossRef](#)] [[PubMed](#)]
62. Cerullo, G.; Polli, D.; Lanzani, G.; De Silvestri, S.; Hashimoto, H.; Cogdell, R.J. Photosynthetic light harvesting by carotenoids: Detection of an intermediate excited state. *Science* **2002**, *298*, 2395–2398. [[CrossRef](#)] [[PubMed](#)]
63. Gitelson, A.A.; Zur, Y.; Chivkunova, O.B.; Merzlyak, M.N. Assessing carotenoid content in plant leaves with reflectance spectroscopy. *Photochem. Photobiol.* **2002**, *75*, 272–281. [[CrossRef](#)]
64. Sarijeva, G.; Knapp, M.; Lichtenthaler, H.K. Differences in photosynthetic activity, chlorophyll and carotenoid levels, and in chlorophyll fluorescence parameters in green sun and shade leaves of ginkgo and fagus. *J. Plant Physiol.* **2007**, *164*, 950–955. [[CrossRef](#)] [[PubMed](#)]

65. Yi, Q.; Jiapaer, G.; Chen, J.; Bao, A.; Wang, F. Different units of measurement of carotenoids estimation in cotton using hyperspectral indices and partial least square regression. *ISPRS J. Photogramm. Remote Sens.* **2014**, *91*, 72–84. [[CrossRef](#)]
66. Marquardt, J. Effects of carotenoid-depletion on the photosynthetic apparatus of a galdieria sulphuraria (rhodophyta) strain that retains its photosynthetic apparatus in the dark. *J. Plant Physiol.* **1998**, *152*, 372–380. [[CrossRef](#)]
67. Shumbe, L.; Bott, R.; Havaux, M. Dihydroactinidiolide, a high light-induced  $\beta$ -carotene derivative that can regulate gene expression and photoacclimation in arabidopsis. *Mol. Plant* **2014**, *7*, 1248–1251. [[CrossRef](#)] [[PubMed](#)]
68. García-Plazaola, J.I.; Portillo-Estrada, M.; Fernández-Marín, B.; Kännaste, A.; Niinemets, Ü. Emissions of carotenoid cleavage products upon heat shock and mechanical wounding from a foliose lichen. *Environ. Exp. Bot.* **2017**, *133*, 87–97. [[CrossRef](#)]
69. Biswal, B. Carotenoid catabolism during leaf senescence and its control by light. *J. Photochem. Photobiol. B Biol.* **1995**, *30*, 3–13. [[CrossRef](#)]
70. Merzlyak, M.N.; Gitelson, A.A.; Chivkunova, O.B.; Rakitin, V.Y. Non-destructive optical detection of pigment changes during leaf senescence and fruit ripening. *Physiol. Plant.* **1999**, *106*, 135–141. [[CrossRef](#)]
71. Price, A.H.; Hendry, G.A.F. Iron-catalysed oxygen radical formation and its possible contribution to drought damage in nine native grasses and three cereals. *Plant Cell Environ.* **1991**, *14*, 477–484. [[CrossRef](#)]
72. Peng, S.; Garcia, F.V.; Laza, R.C.; Sanico, A.L.; Visperas, R.M.; Cassman, K.G. Increased N-use efficiency using a chlorophyll meter on high-yielding irrigated rice. *Field Crop. Res.* **1996**, *47*, 243–252. [[CrossRef](#)]
73. Vázquez-Durán, A.; Araujo-Andrade, C.; Castañón, G.M.; Ortega-Zarzosa, G.; Ruiz, F.; Martínez, J.R. Spectral characterization of chlorophyll fluorescence in extract of barley leaves embedded in silica xerogel matrix. *J. Sol-Gel Sci. Technol.* **2006**, *39*, 223–227. [[CrossRef](#)]
74. Fernández-Marín, B.; Artetxe, U.; Barrutia, O.; Esteban, R.; Hernández, A.; García-Plazaola, J.I. Opening Pandora's box: Cause and impact of errors on plant pigment studies. *Front. Plant Sci.* **2015**, *6*, 148. [[CrossRef](#)] [[PubMed](#)]
75. Markwell, J.; Osterman, J.C.; Mitchell, J.L. Calibration of the Minolta SPAD-502 leaf chlorophyll meter. *Photosynth. Res.* **1995**, *46*, 467–472. [[CrossRef](#)] [[PubMed](#)]
76. Yamamoto, A.; Nakamura, T.; Adu-Gyamfi, J.J.; Saigusa, M. Relationship between chlorophyll content in leaves of sorghum and pigeonpea determined by extraction method and by chlorophyll meter (SPAD-502). *J. Plant Nutr.* **2002**, *25*, 2295–2301. [[CrossRef](#)]
77. Netto, A.T.; Campostrini, E.; de Oliveira, J.G.; Bressan-Smith, R.E. Photosynthetic pigments, nitrogen, chlorophyll a fluorescence and SPAD-502 readings in coffee leaves. *Sci. Hortic.* **2005**, *104*, 199–209. [[CrossRef](#)]
78. Nauš, J.; Prokopová, J.; Řebíček, J.; Špundová, M. SPAD chlorophyll meter reading can be pronouncedly affected by chloroplast movement. *Photosynth. Res.* **2010**, *105*, 265–271. [[CrossRef](#)] [[PubMed](#)]
79. Yuan, Z.; Cao, Q.; Zhang, K.; Ata-Ul-Karim, S.T.; Tian, Y.; Zhu, Y.; Cao, W.; Liu, X. Optimal leaf positions for SPAD meter measurement in rice. *Front. Plant Sci.* **2016**, *7*, 719. [[CrossRef](#)] [[PubMed](#)]
80. Uddling, J.; Gelang-Alfredsson, J.; Piikki, K.; Pleijel, H. Evaluating the relationship between leaf chlorophyll concentration and SPAD-502 chlorophyll meter readings. *Photosynth. Res.* **2007**, *91*, 37–46. [[CrossRef](#)] [[PubMed](#)]
81. Marengo, R.A.; Antezana-Vera, S.A.; Nascimento, H.C.S. Relationship between specific leaf area, leaf thickness, leaf water content and SPAD-502 readings in six Amazonian tree species. *Photosynthetica* **2009**, *47*, 184–190. [[CrossRef](#)]
82. Parry, C.; Blonquist, J.M.; Bugbee, B. In situ measurement of leaf chlorophyll concentration: Analysis of the optical/absolute relationship. *Plant Cell Environ.* **2014**, *37*, 2508–2520. [[CrossRef](#)] [[PubMed](#)]
83. Lin, C.; Popescu, S.C.; Huang, S.C.; Chang, P.T.; Wen, H.L. A novel reflectance-based model for evaluating chlorophyll concentrations of fresh and water-stressed leaves. *Biogeosciences* **2015**, *12*, 49–66. [[CrossRef](#)]
84. Xiong, D.; Chen, J.; Yu, T.; Gao, W.; Ling, X.; Li, Y.; Peng, S.; Huang, J. SPAD-based leaf nitrogen estimation is impacted by environmental factors and crop leaf characteristics. *Sci. Rep.* **2015**, *5*, 13389. [[CrossRef](#)] [[PubMed](#)]
85. Kitajima, K.; Hogan, K.P. Increases of chlorophyll a/b ratios during acclimation of tropical woody seedlings to nitrogen limitation and high light. *Plant Cell Environ.* **2003**, *26*, 857–865. [[CrossRef](#)] [[PubMed](#)]

86. Maina, J.N.; Wang, Q. Seasonal response of chlorophyll a/b ratio to stress in a typical desert species: *Haloxylon ammodendron*. *Arid Land Res. Manag.* **2015**, *29*, 321–334. [[CrossRef](#)]
87. Yang, S.L.; Yano, T.; Aydin, M.; Kitamura, Y.; Takeuchi, S. Short term effects of saline irrigation on evapotranspiration from lysimeter-grown citrus trees. *Agric. Water Manag.* **2002**, *56*, 131–141. [[CrossRef](#)]
88. Sims, D.A.; Gamon, J.A. Relationships between leaf pigment content and spectral reflectance across a wide range of species, leaf structures and developmental stages. *Remote Sens. Environ.* **2002**, *81*, 337–354. [[CrossRef](#)]
89. Zhang, S.; Ma, K.; Chen, L. Response of photosynthetic plasticity of *paeonia suffruticosa* to changed light environments. *Environ. Exp. Bot.* **2003**, *49*, 121–133. [[CrossRef](#)]
90. García-Valenzuela, X.; García-Moya, E.; Rascón-Cruz, Q.; Herrera-Estrella, L.; Aguado-Santacruz, G.A. Chlorophyll accumulation is enhanced by osmotic stress in graminaceous chlorophyll cells. *J. Plant Physiol.* **2005**, *162*, 650–661. [[CrossRef](#)] [[PubMed](#)]
91. Ciganda, V.; Gitelson, A.; Schepers, J. Vertical profile and temporal variation of chlorophyll in maize canopy: Quantitative “crop vigor” indicator by means of reflectance-based techniques. *Agron. J.* **2008**, *100*, 1409–1417. [[CrossRef](#)]
92. Li, J.W.; Yang, J.P.; Fei, P.P.; Song, J.L.; Li, D.S.; Ge, C.S.; Chen, W.Y. Responses of rice leaf thickness, spad readings and chlorophyll a/b ratios to different nitrogen supply rates in paddy field. *Field Crop. Res.* **2009**, *114*, 426–432.
93. Porcar-Castell, A.; Tyystjarvi, E.; Atherton, J.; van der Tol, C.; Flexas, J.; Pfundel, E.E.; Moreno, J.; Frankenberg, C.; Berry, J.A. Linking chlorophyll a fluorescence to photosynthesis for remote sensing applications: Mechanisms and challenges. *J. Exp. Bot.* **2014**, *65*, 4065–4095. [[CrossRef](#)] [[PubMed](#)]
94. Jiang, Y.; Ding, X.; Zhang, D.; Deng, Q.; Yu, C.-L.; Zhou, S.; Hui, D. Soil salinity increases the tolerance of excessive sulfur fumigation stress in tomato plants. *Environ. Exp. Bot.* **2017**, *133*, 70–77. [[CrossRef](#)]
95. Bizhani, S.; Salehi, H. Physio-morphological and structural changes in common bermudagrass and kentucky bluegrass during salt stress. *Acta Physiol. Plant.* **2014**, *36*, 777–786. [[CrossRef](#)]
96. Gómez-Bellot, M.J.; Nortes, P.A.; Ortuño, M.F.; Romero, C.; Fernández-García, N.; Sánchez-Blanco, M.J. Influence of arbuscular mycorrhizal fungi and treated wastewater on water relations and leaf structure alterations of *viburnum tinus* L. Plants during both saline and recovery periods. *J. Plant Physiol.* **2015**, *188*, 96–105. [[CrossRef](#)] [[PubMed](#)]
97. García-Sánchez, F.; Jifon, J.L.; Carvajal, M.; Syvertsen, J.P. Gas exchange, chlorophyll and nutrient contents in relation to Na<sup>+</sup> and Cl<sup>-</sup> accumulation in ‘sunburst’ mandarin grafted on different rootstocks. *Plant Sci.* **2002**, *162*, 705–712. [[CrossRef](#)]
98. Pandolfi, C.; Mancuso, S.; Shabala, S. Physiology of acclimation to salinity stress in pea (*pisum sativum*). *Environ. Exp. Bot.* **2012**, *84*, 44–51. [[CrossRef](#)]
99. Higbie, S.M.; Wang, F.; Stewart, J.M.; Sterling, T.M.; Lindemann, W.C.; Hughs, E.; Zhang, J. Physiological response to salt (nacl) stress in selected cultivated tetraploid cottons. *Int. J. Agron.* **2010**, *2010*, 12. [[CrossRef](#)]
100. Stefanov, M.; Yotsova, E.; Rashkov, G.; Ivanova, K.; Markovska, Y.; Apostolova, E.L. Effects of salinity on the photosynthetic apparatus of two paulownia lines. *Plant Physiol. Biochem.* **2016**, *101*, 54–59. [[CrossRef](#)] [[PubMed](#)]
101. Khatkar, D.; Kuhad, M.S. Short-term salinity induced changes in two wheat cultivars at different growth stages. *Biol. Plant.* **2000**, *43*, 629–632. [[CrossRef](#)]
102. Stepien, P.; Johnson, G.N. Contrasting responses of photosynthesis to salt stress in the glycophyte *arabidopsis* and the halophyte *thellungiella*: Role of the plastid terminal oxidase as an alternative electron sink. *Plant Physiol.* **2009**, *149*, 1154–1165. [[CrossRef](#)] [[PubMed](#)]
103. Aspelmeier, S.; Leuschner, C. Genotypic variation in drought response of silver birch (*betula pendula roth*): Leaf and root morphology and carbon partitioning. *Trees* **2006**, *20*, 42–52. [[CrossRef](#)]
104. Marron, N.; Dreyer, E.; Boudouresque, E.; Delay, D.; Petit, J.-M.; Delmotte, F.M.; Brignolas, F. Impact of successive drought and re-watering cycles on growth and specific leaf area of two *populus × canadensis* (moench) clones, ‘dorskamp’ and ‘luisa\_avanzo’. *Tree Physiol.* **2003**, *23*, 1225–1235. [[CrossRef](#)] [[PubMed](#)]
105. Pessarakli, M.; Tucker, T.C. Nitrogen-15 uptake by eggplant under sodium chloride stress. *Soil Sci. Soc. Am. J.* **1988**, *52*, 1673–1676. [[CrossRef](#)]

106. Syvertsen, J.; Lloyd, J.; Kriedemann, P. Salinity and drought stress effects on foliar ion concentration, water relations, and photosynthetic characteristics of orchard citrus. *Aust. J. Agric. Res.* **1988**, *39*, 619–627. [[CrossRef](#)]
107. Zhu, J.K. Plant salt tolerance. *Trends Plant Sci.* **2001**, *6*, 66–71. [[CrossRef](#)]
108. Parida, A.K.; Das, A.B. Salt tolerance and salinity effects on plants: A review. *Ecotoxicol. Environ. Saf.* **2005**, *60*, 324–349. [[CrossRef](#)] [[PubMed](#)]
109. Silveira, J.A.G.; Silva, E.N.; Ferreira-Silva, S.L.; Viégas, R.A. Physiological mechanisms involved with salt and drought tolerance in *jatropha curcas* plants. In *Jatropha, Challenges for A New Energy Crop: Volume 1: Farming, Economics and Biofuel*; Springer: New York, NY, USA, 2012; pp. 125–152.
110. Gaborcik, N. Relationship between contents of chlorophyll (a+b) (spad values) and nitrogen of some temperate grasses. *Photosynthetica* **2003**, *41*, 285–287. [[CrossRef](#)]
111. Gitelson, A.A.; Gritz, Y.; Merzlyak, M.N. Relationships between leaf chlorophyll content and spectral reflectance and algorithms for non-destructive chlorophyll assessment in higher plant leaves. *J. Plant Physiol.* **2003**, *160*, 271–282. [[CrossRef](#)] [[PubMed](#)]
112. Gitelson, A.A.; Peng, Y.; Arkebauer, T.J.; Schepers, J. Relationships between gross primary production, green lai, and canopy chlorophyll content in maize: Implications for remote sensing of primary production. *Remote Sens. Environ.* **2014**, *144*, 65–72. [[CrossRef](#)]
113. Campbell, E.E.; Knoop, W.T.; Bate, G.C. A comparison of phytoplankton biomass and primary production in three eastern cape estuaries, south africa. *S. Afr. J. Sci.* **1991**, *87*, 259–264.
114. Houborg, R.; Anderson, M.; Daughtry, C. Utility of an image-based canopy reflectance modeling tool for remote estimation of lai and leaf chlorophyll content at the field scale. *Remote Sens. Environ.* **2009**, *113*, 259–274. [[CrossRef](#)]
115. Wellburn, A.R. The spectral determination of chlorophylls a and b, as well as total carotenoids, using various solvents with spectrophotometers of different resolution. *J. Plant Physiol.* **1994**, *144*, 307–313. [[CrossRef](#)]
116. Liu, L.-Y.; Huang, W.-J.; Pu, R.-L.; Wang, J.-H. Detection of internal leaf structure deterioration using a new spectral ratio index in the near-infrared shoulder region. *J. Integr. Agric.* **2014**, *13*, 760–769. [[CrossRef](#)]
117. Poljakoff-Mayber, A.; Bar-Nun, N.; Hasson, E.; Heichal, O. Respiratory carbohydrate metabolism of different pea varieties under saline conditions. *Bot. Gaz.* **1981**, *142*, 431–437. [[CrossRef](#)]
118. Andrea, B.; Tani, C. Ultrastructural effects of salinity in nicotiana bigelovii var. Bigelovii callus cells and allium cepa roots. *Caryologia* **2009**, *62*, 124–133. [[CrossRef](#)]
119. Kalaji, H.M.; Dąbrowski, P.; Cetner, M.D.; Samborska, I.A.; Łukasik, I.; Brestic, M.; Zivcak, M.; Tomasz, H.; Mojski, J.; Kociel, H.; et al. A comparison between different chlorophyll content meters under nutrient deficiency conditions. *J. Plant Nutr.* **2017**, *40*, 1024–1034. [[CrossRef](#)]
120. Evelin, H.; Giri, B.; Kapoor, R. Ultrastructural evidence for amf mediated salt stress mitigation in trigonella foenum-graecum. *Mycorrhiza* **2013**, *23*, 71–86. [[CrossRef](#)] [[PubMed](#)]
121. Rahman, S.; Matsumuro, T.; Miyake, H.; Takeoka, Y. Salinity-induced ultrastructural alterations in leaf cells of rice (*oryza sativa* L.). *Plant Prod. Sci.* **2000**, *3*, 422–429. [[CrossRef](#)]
122. Baker, C.S.; Dunn, M.J.; Yacoub, M.H. Evaluation of membranes used for electroblotting of proteins for direct automated microsequencing. *Electrophoresis* **1991**, *12*, 342–348. [[CrossRef](#)] [[PubMed](#)]
123. Bashour, I.I.; Al-Mashhady, A.S.; Devi Prasad, J.; Miller, T.; Mazroa, M. Morphology and composition of some soils under cultivation in saudi arabia. *Geoderma* **1983**, *29*, 327–340. [[CrossRef](#)]
124. Steduto, P.; Hsiao, T.C.; Raes, D.; Fereres, E. Aquacrop—the fao crop model to simulate yield response to water: I. Concepts and underlying principles. *Agron. J.* **2009**, *101*, 426–437. [[CrossRef](#)]
125. Benbella, M.; Paulsen, G.M. Efficacy of treatments for delaying senescence of wheat leaves: II. Senescence and grain yield under field conditions. *Agron. J.* **1998**, *90*, 332–338. [[CrossRef](#)]
126. Arnon, D.I. Copper enzymes in isolated chloroplasts. Polyphenoloxidase in beta vulgaris. *Plant Physiol.* **1949**, *24*, 1. [[CrossRef](#)] [[PubMed](#)]
127. Rocha, A.V.; Shaver, G.R. Advantages of a two band evi calculated from solar and photosynthetically active radiation fluxes. *Agric. For. Meteorol.* **2009**, *149*, 1560–1563. [[CrossRef](#)]

128. Tukey, J.W. *Exploratory Data Analysis*; Addison-Wesley: Boston, MA, USA, 1977; p. 704.
129. Noru, M.J. *Ibm Spss Statistics 19 Guide to Data Analysis*; Prentice Hall: Upper Saddle River, NJ, USA, 2012.



© 2017 by the authors. Licensee MDPI, Basel, Switzerland. This article is an open access article distributed under the terms and conditions of the Creative Commons Attribution (CC BY) license (<http://creativecommons.org/licenses/by/4.0/>).